Scaling Law for Entropic Effects at Interfaces between Grafted Layers and Polymer Melts

Paula G. Ferreira* and Armand Ajdari

Laboratoire de Physico-Chimie Théorique, ESPCI, 10 Rue Vauquelin, 75231 Paris Cedex 05, France

Ludwik Leibler

Unité Mixte de Recherche CNRS-Elf Atochem (UMR 167), 95 Rue Danton, BP 108, 92303 Levallois-Perret Cedex, France

Received August 18, 1997; Revised Manuscript Received April 9, 1998

ABSTRACT: We consider surfaces protected by polymer chains of N monomers grafted at a density σ, that are immersed in a melt of chemically similar chains of polymerization index P. We have used the self-consistent field approximation to analyze the practically useful (but analytically untractable) case of moderately long melt chains and moderately stretched grafted chains. We have confirmed previous analyses of concentration profiles, but we have also arrived at new features by looking in a systematic way at the interaction energy between two grafted surfaces: (i) we have found a general scaling criterion that an entropic attraction between two such surfaces exists if $\sigma\sqrt{N} > (N/P)^2$, which differs from predictions obtained for very stretched brushes; (ii) this work also demonstrates the existence of an attraction for sparsely grafted layers ($\sigma\sqrt{N} < 1$) provided that P is large enough. These subtle entropic effects should be of direct consequence for "macroscopic" phenomena such as wetting of protected surfaces and colloidal stabilization.

I. Introduction

Macroscopic phenomena of technological importance in polymer systems can be induced by subtle microscopic entropic effects due to topological constraints. An interesting case is that of the interface between a brush and a melt of chemically similar chains. Because of the constraints on the brush chains, an effective positive surface tension arises. This can directly induce partial wetting of a melt on a chemically identical surface (sometimes referred to as autophobicity)[1−8] or indirectly provoke the effective attraction of two brushes in a melt, resulting, for example, in the flocculation of protected colloidal particles[9] or micelle aggregation and phase separation in homopolymer−copolymer mixtures.[10,11]

Theoretically, one has to deal with a complex problem specified by three parameters: N and P, the polymerization indices of the brush and melt chains, respectively, and σ, the grafting density of the brush. Most existing analyses have focused on the analytically solvable limits of densely grafted brushes, $\sigma\sqrt{N} \gg 1$, and either very short ($P \ll N$) or very long melt chains ($P \gg N$).[1,2,9,10,12] In these regimes, the study of subtle second-order effects leads to scaling laws for the thickness of the brush−melt interpenetration region, λ, and for the effective surface tension γ in terms of N, P, and σ. These analyses were rather successful in providing qualitative prediction and interpretation of experimental observations.[1−7]

However, most experimentally interesting systems are far from these limiting regimes: P and N are typically of the same order, and the grafted layers are seldom very stretched. For such systems it becomes necessary to use numerical methods, the most accurate being the self-consistent field (SCF) approximation. This method has recently led to results for the interface structure that agree qualitatively with the theoretical predictions, although the parameters used were somewhat away from the strict domain of validity of the analytical studies.[9,13] More recently, a study has shown that the agreement was not so good for the scaling dependence of energies on the parameters.[9]

In this paper, using a continuous 1D SCF theory, we perform a more systematic exploration of the parameter space of a polymer protected surface in contact with a melt, calculating both concentration profiles and energies, to answer questions such as: For what parameters is there an effective attraction between two grafted surfaces? Are there scaling laws that allow one to rationalize this behavior in these intermediate regimes and thus provide us with simple criteria? Actually, we will show that the domain where attraction exists between two grafted layers, and where partial wetting is thus expected, can indeed be simply described by $\sigma\sqrt{N} > (N/P)^2$. For dense brushes ($\sigma\sqrt{N} > 1$) this criterion is slightly different from the crossover between the two predicted regimes for the interpenetration thickness λ. For sparsely grafted layers ($\sigma\sqrt{N} < 1$) it corresponds to a qualitatively new attraction scenario, unaccessible by asymptotic theories for stretched brushes.

This paper is organized as follows. In the remainder of this Introduction we recall briefly some theoretical and experimental results associated with the existence of a positive surface tension between the melt and grafted layers. In section II we present the SCF formalism. Section III contains our results organized in the following way: we first analyze concentration profiles and obtain agreement with previous studies; we then turn to the interaction of two grafted surfaces and analyze the more "classic" case of somewhat stretched layers ($\sigma\sqrt{N} > 1$), before turning to the previously undiscussed case of sparse layers ($\sigma\sqrt{N} < 1$). A brief discussion of the practical consequences of our work is presented with the conclusions in section IV.

S0024-9297(97)01246-1 CCC: $15.00
Published on Web 05/23/1998

The existence of a positive surface tension inducing an autophobic wetting behavior in polymeric liquids was theoretically predicted by Leibler et al.,[1,2] using free energy balance arguments, for the case of a melt of very long chains $P \gg N$. This autophobic behavior of the polymer chains was tested experimentally, and the measured value for the contact angle of the equilibrium droplets was found to be in good agreement with the expected one.[1,2] Several other experimental results that exemplify the autophobic wetting behavior of the polymer chains were obtained by different groups.[3−7] The related phenomena of dewetting of a polymer melt on top of a cross-linked network was also observed recently.[14] Numerical simulation results of Binder et al.[15] have shown the expulsion of a free chain from a dense layer of grafted chains. A different theoretical approach to this problem was proposed by Shull,[8] who used the SCF theory to show that for end-adsorbed polymers in chemically identical polymer matrixes, when $P > N$, the Helmholtz free energy is able to describe dewetting in the frame of the Brochard−Wyart continuum picture.[16]

The study of the interface between a grafted layer and a bulk melt of chemically identical chains is not a new problem. It started well before the phenomena of autophobicity was first discussed. It dates back to 1980, to the pioneering work of de Gennes on brushes.[17] The problem is treated there in the case where the grafted chains are in contact with a melt of shorter chemically identical chains ($P < N$). A scaling analysis yields a description of the brush height h, according to the different regimes of behavior that can be found in the space of the parameters N, P, and grafting density of the brush, σ. Some years later, Witten et al.[18] and Zhulina et al.[19] described the scaling dependency of the interpenetration of the melt free polymer and the grafted layer, λ. In a later work[13] those scaling laws for λ and h were compared with the numerical results of the SCFT and the agreement found was good. A diagram of state, with the regions with different scaling behaviors of h and λ, was also shown both for $P < N$ and for $P > N$ in this same work. More recently, equivalent scaling laws for the width of the brush−melt interface at large grafting densities and large values of P were obtained by Gay.[12] Some of the results of Leibler et al.[1] for $P \gg N$ are recovered in this work. In his work Gay also comments, for the first time, on the connection between the expulsion of the free chains from the grafted layer (described by the scaling laws mentioned above) and the appearance of a positive surface tension between the grafted polymer chains and the melt. In the works of Shull[20,21] an extended analysis of a brush immersed in a melt is done for the case $P > N$ and experimental profiles are compared with numerical SCF results. No attempt is made, however, to characterize the locus of (N, P, σ) points that define the transition between the dry and the wet brush regimes. Moreover, the system they studied is not the same as ours since they consider an end-adsorbed layer in thermodynamic equilibrium with the bulk matrix. The grafting density σ, is not an independent external parameter of their system, as discussed in ref 8.

The positive surface tension that is at the basis of autophobicity is also the mechanism responsible for the existence, under certain conditions, of an effective entropic attraction between brushy aggregates and polymer protected particles in a melt of long chains, as suggested in refs 1, 2, and 9−11. If the brush−melt interfacial tension is positive, the system would rather prefer to replace the two brush−melt interfaces by a single brush−brush interface. In the past decade, SCF theory results have been obtained, by several different groups, for the attractive minimum that appears in the interaction free energy of two brushes immersed in a melt (or in a polymer solution).[13,20,22] A global interpretation of these results is, however, missing, and the influence of several parameters (N, P, σ, and concentration of free polymer) is not always clear. At best, it is recognized that the minimum appears only when the free polymer chain length exceeds a certain critical value that depends, in an unknown way, on the length of the grafted polymer chain and on the grafting density of the brush.

Recently, experimental results have been reported on the existence of an optimum grafting density for dispersing particles in polymer melts.[9] It is shown that grafting polymers on the particles will enhance their dispersion if the grafting density is low, but it will cause their flocculation when σ becomes too high. The existence of an attractive part in the surface force between the particles for high values of σ provides an explanation of these experimental results. At low σ, van der Waals attraction between the particles dominates and increasing the number of grafted chains will improve the dispersion due to the repulsion of the grafted layers. However, for high enough values of the grafting density the effective entropic attraction between the grafted layers appears and the dispersion worsens. In ref 9 the authors used the SCF approximation to compute the interaction force between the polymer-protected particles in the melt and discuss the appearance of this attractive part. For grafted and matrix polymers of polymerization index $N \simeq P = 100$, the optimum grafting density they obtained was $\sigma = 0.1$, a value that agrees well with their experimental results. They estimated that in the case $N \simeq P$ the optimum grafting density should behave like $\sigma \simeq 1/\sqrt{N}$. Their analysis was, however, restricted to that particular set of parameters.

II. Formalism

In this section the presentation of the formalism will follow ref 23, where a more detailed description of the SCF approximation can be found.

We consider a polymer melt of n_α chains with polymerization index P in contact with a substrate covered by a densely grafted layer of n_β chains with polymerization index N and grafting density σ. The polymers are confined to a box of volume V with a surface of area S, located at $z = 0$, at which the polymers were grafted. The grafting density is defined as $\sigma = n_\beta/S$. The only allowed trajectories of the polymer chains belong to the region $0 < z < z_{max}$, where $z_{max} = V/S$. We assume that the properties of the system are only a function of the distance to the substrate. Translational invariance is implicitly assumed in the planes parallel to the grafting surface. At sufficiently large values of z, the influence of the brush ceases to exist and the P melt chains attain their bulk properties. The bulk is characterized by a constant mean density of monomers $\phi_0 = 1$.

Each polymer $\alpha = 1, ..., n_\alpha$, $\beta = 1, ..., n_\beta$ is modeled as a flexible chain that is described by a curve $z_\alpha(t)$ or $z_\beta(t)$ representing all possible configurations of the macromolecules. The variable t increases continuously along the length of the chain. For the grafted chains, $t = 0$

at the grafting wall and $t = N$ at its free extremity. In the case of the bulk chains the two extremities are naturally equivalent. The probability density functional for a given space curve is assumed to be of the Wiener form

$$P\,[z_\alpha] \propto \exp\left[-\frac{3}{2a^2}\int_0^P \mathrm{d}t\left|\frac{\mathrm{d}z_\alpha(t)}{\mathrm{d}t}\right|^2\right] \tag{1}$$

and $P\,[z_\beta]$ is given by a similar expression with P replaced by N. In this equation a is the Kuhn length of the monomers, assumed to be the same for both grafted and mobile chains. This functional describes the intramolecular bonding of the chains.

Thermodynamic equilibrium of the P melt chains close to the grafted layer is obtained when the chemical potential is uniform along the z direction and equal to its bulk value. There is no reason, however, to impose this chemical potential on the grafted polymers of the brush. For a given N, the state of the brush is completely determined by the value of the grafting density, σ. The brush is going to act like a surface constraint for the bulk melt. This is the basic difference between our work and that of ref 20.

The grand canonical partition function for the system can thus be written as

$$Z_\mu = \sum_{n_\alpha=0}^{\infty} \mathrm{e}^{n_\alpha P\mu} Z_{n_\alpha, n_\beta} \tag{2}$$

where μ is the chemical potential per monomer and Z_{n_α,n_β} is the canonical partition function for n_α free polymers and n_β grafted polymers in the box:

$$Z_{n_\alpha,n_\beta} = \frac{1}{n_\alpha!}\frac{1}{n_\beta!}\prod_{\alpha=1}^{n_\alpha}\int Dz_\alpha\, P\,[z_\alpha] \times \prod_{\beta=1}^{n_\beta}\int Dz_\beta\, P\,[z_\beta]\, \delta[1 - \hat{\phi}_\alpha - \hat{\phi}_\beta] \tag{3}$$

Here the integrals in Dz_α and Dz_β denote the functional integrals over all possible configurations of the chains. The δ functional selects out the configurations satisfying the incompressibility constraint of the melt. An explicit interaction potential between the grafted and free chains is not considered since we have assumed that all the polymers have the same chemical nature. The monomer density operators $\hat{\phi}_\alpha$ and $\hat{\phi}_\beta$ are defined as

$$\hat{\phi}_\alpha(z) = \sum_{\alpha=1}^{n_\alpha}\int_0^P \mathrm{d}t\, \delta(z - z_\alpha(t)) \tag{4a}$$

$$\hat{\phi}_\beta(z) = \sum_{\beta=1}^{n_\beta}\int_0^N \mathrm{d}t\, \delta(z - z_\beta(t)) \tag{4b}$$

To replace the operators $\hat{\phi}$ by the functions ϕ, one inserts in eq 3 of the canonical partition function the functional integrals $1 = \int D\phi_\alpha\, \delta[\phi_\alpha - \hat{\phi}_\alpha]$ and $1 = \int D\phi_\beta\, \delta[\phi_\beta - \hat{\phi}_\beta]$.[24,25] Using the integral representation of the δ functionals, where N is a normalization constant

$$\delta(\phi - \hat{\phi}) = N\int_{-i\infty}^{i\infty} \mathrm{d}W\, \mathrm{e}^{\int \mathrm{d}_z W(z)(\phi(z) - \hat{\phi}(z))} \tag{5}$$

the grand canonical partition function can finally be written in terms of the fields W_α, W_β, and ξ as

$$Z_\mu = N\int D\phi_\alpha\, D\phi_\beta\, DW_\alpha\, DW_\beta\, D\xi \times \mathrm{e}^{\int \mathrm{d}z(W_\alpha\phi_\alpha + W_\beta\phi_\beta + \xi(1 - \phi_\alpha - \phi_\beta))}\prod_{\beta=1}^{n_\beta}\frac{Q_\beta}{n_\beta!}\sum_{n_\alpha=0}^{\infty}\mathrm{e}^{n_\alpha P\mu}\prod_{\alpha=1}^{n_\alpha}\frac{Q_\alpha}{n_\alpha!} \tag{6}$$

The SCF approximation is a mean field theory where the many interacting chains problem is reduced to that of independent chains subject to an external (mean) field, created by the other chains. The Q_α and Q_β are the individual canonical partition functions of the noninteracting α and β chains in the external fields W_α and W_β.

$$Q_\alpha = \int Dz_\alpha\, P\,[z_\alpha]\, \mathrm{e}^{-\int_0^P \mathrm{d}t W_\alpha[z_\alpha(t)]} \tag{7}$$

The expression for Q_β is similar, with P replaced by N. Since all α chains are equivalent between themselves and the same happens with the β chains, the product of the n_α and n_β individual partition functions in eq 6 can simply be replaced by $Q_\alpha^{n_\alpha}$ and $Q_\beta^{n_\beta}$.

If we define the individual grand canonical partition function of the mobile P chains in the external field W as

$$\Omega\mu[\mathrm{W}] = \sum_{n=0}^{\infty}\mathrm{e}^{nP\mu}\frac{Q^n}{n!} \tag{8}$$

we can rewrite eq 6 in the form

$$Z_\mu = N\int D\phi_\alpha\, D\phi_\beta\, DW_\alpha\, DW_\beta\, D\xi\, \mathrm{e}^{-\beta F} \tag{9a}$$

$$\beta F = -\int \mathrm{d}z\, (W_\alpha(z)\,\phi_\alpha(z) + W_\beta(z)\,\phi_\beta(z) + \xi(z)(1 - \phi_\alpha(z) - \phi_\beta(z))) - n_\beta \log\frac{Q_\beta}{n_\beta!} - \log\Omega_\mu[W_\alpha] \tag{9b}$$

Equations 9 for the grand canonical partition function are exact and, like the initial expression (2), cannot be computed exactly. Although for a given set of fields, $\Omega_\mu[W_\alpha]$ and Q_β could be calculated, the functional integrals in ϕ_α, ϕ_β, W_α, W_β, and ξ cannot be done. In the SCFT, a saddle point approximation is used and the integral in eq 9b is approximated by the extremum value of the integrand.

Doing the variation with respect to ϕ_α, ϕ_β, ξ, W_α, and W_β, respectively, we obtain the set of self-consistent equations for the density profiles and for the mean fields:

$$W_\alpha(z) = \xi(z) \tag{10a}$$

$$W_\beta(z) = \xi(z) \tag{10b}$$

$$\phi_\alpha(z) + \phi_\beta(z) = 1 \tag{10c}$$

$$\phi_\alpha(z) = -\mathrm{e}^{P\mu}\frac{DQ_\alpha}{DW_\alpha} \tag{10d}$$

$$\phi_\beta = -\frac{n_\beta}{Q_\beta}\frac{DQ_\beta}{DW_\beta} \tag{10e}$$

where in eq 10d we have used the identity

$$\frac{D\,\log\Omega_\mu[W]}{DW} = \mathrm{e}^{P\mu}\frac{DQ}{DW}$$

Once the partition functions Q_α and Q_β are known, eqs 10 can be solved. It is possible[26,27] to write the partition function Q in terms of the end monomer distribution functions $q(z_f,z_i;N)$ or $q(z_f;N)$ that represent the probability that a chain ends at z_f in N steps having started at z_i, or regardless of where it starts:

$$Q = \int dz_f \int dz_i\, q(z_f,z_i;N) = \int dz_f\, q(z_f;N) \quad (11)$$

The distribution functions satisfy a modified diffusion equation:

$$\frac{\partial q}{\partial \mathbf{t}} = \frac{a^2}{6}\frac{\partial^2 q}{\partial z^2} - Wq \quad (12)$$

with initial condition $q(z_f,z_i;0) = \delta(z_f - z_i)$, or equivalently $q(z_f;0) = 1$.

One can rewrite eqs 10d and 10e for the monomer density in terms of the propagators q so defined, as

$$\phi_\alpha(z) = e^{P\mu}\int_0^P dt\, q_\alpha(z;t)\, q_\alpha(z;P-t) \quad (13a)$$

and

$$\phi_\beta = n_\beta \frac{\int_0^N dt\, q_\beta(z;t)\, q_\beta(z;N-t)}{\int dz\, q_\beta(z;N)} \quad (13b)$$

A point along a given polymer chain is characterized by the diffusion paths from the two chain ends. In the case of the α bulk chains the two extremities are equivalent and one propagator is sufficient to describe the system. Since the bulk chain ends can be found everywhere inside the box, the initial condition for the q_α propagator is $q_\alpha(z;t=0) = 1$, $\forall z \in]0, z_{max}[$. This is no longer true for the β grafted chains. In a brush, the two extremities are distinct and we need two different propagators q_β and q_β^+ to characterize the diffusion paths starting from the grafted and the free chain end. We will have the initial conditions $q_\beta(z=0;t=0) = 1$ and $q_\beta^+(z;t=N) = 1$, $\forall z \in]0, z_{max}[$.

The boundary conditions $q_\beta(z<0;t) = q_\beta^+(z<0;t) = 0$ and $q_\beta(z>z_{max};t) = q_\beta^+(z>z_{max};t) = 0$ that describe the confinement of the chains inside the box are used for the brush propagators. For the mobile chains we have, in a similar way, $q_\alpha(z<0;t)$. For large values of z the P melt chains attain their bulk properties. At $z = z_{max}$ the mean density of monomers is already uniform, $\phi_\alpha(z \geq z_{max}) = \phi_0 = 1$ and the propagator is no longer a position dependent function, $q_\alpha(z;t) = q_0(t)$. Due to the initial condition, $q_0(t)$ has the form $q_0(t) = e^{-W_\alpha t}$, which reduces to $q_0(t) = 1$ in the case of a potential that is zero in the bulk. We have the boundary condition $q_\alpha(z>z_{max};t) = 1$ for the mobile chains.

The equilibrium chemical potential of the free chains μ and the value of the bulk density ϕ_0 are not independent. In order that $\lim_{z\to z_{max}} \phi_\alpha(z) = \phi_0$, the chemical potential has to satisfy $e^{\mu P} = \phi_0/P$.

The mean field $\xi(z)$ that is going to impose the melt incompressibility was chosen to be

$$\xi(z) = \xi(1 - \phi_\alpha(z) - \phi_\beta(z)) \quad (14)$$

with ξ a constant with a high enough value to ensure that, in practice, $\phi_\alpha(z) + \phi_\beta(z) = 1$ and that the resulting density profiles and energies were independent of its particular value. Moreover, this choice enables us to obtain a contribution to the equilibrium free energy with a form similar to that usually found in the literature (see for instance ref 11).

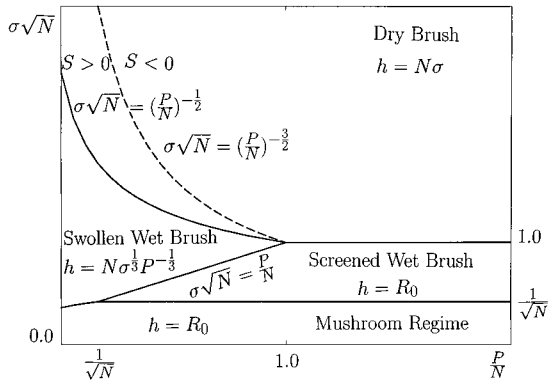

Figure 1. Diagram of state (N, P, σ) according to the scaling laws of refs 12, 13, and 17 of a polymer brush of polymerization index N immersed in a melt of the same polymer with a different polymerization index P. The full lines are the boundaries between the regions with different scaling laws for the brush height, h. The dashed line separates the two regimes of scaling of the brush−melt interfacial thickness and coincides with the frontier between the regions of positive and negative spreading coefficient of refs 1 and 2.

The set of coupled equations for the fields (eqs 10a, 10b, and 14), densities (eqs 13), and propagators (eq 12) was numerically solved in a self-consistent manner using a Picard iteration method. A simple, fully explicit finite-differencing algorithm was used to solve the modified diffusion equation. We work in units of length such that a is unity. The z and t variables were discretized in a rectangular grid with steps $\Delta t = \Delta Z = 0.5$ that were chosen in order to satisfy the stability criterion of the finite-difference approximation to the differential equation.[23]

III. Results

The diagram of state (N, P, σ), according to the scaling laws of refs 12, 13, and 17, of a polymer brush of polymerization index N immersed in a melt of the same polymer with a different polymerization index P is shown in Figure 1. The full lines are the boundary between the regions with different scaling laws for the brush height, h. The dashed line separates the two regimes of scaling of the width of the brush−melt interface, λ, and coincides with the frontier between the regions of positive and negative spreading coefficient of refs 1 and 2.

When the grafting density is small, the chains hardly touch each other and behave like isolated coils. In this mushroom regime the height of the brush is of the order of R_0, the Flory radius of the coil. For an N polymer chain in a P melt the interactions are screened and the swelling of the coil behaves like $h = R_0 = N^{3/5}P^{-1/5}$. When $P/N \geq 1/\sqrt{N}$, the interactions are completely screened and the chain becomes ideal with $h = R_0 = N^{1/2}$. The chains start to interact and the mushroom regime ceases to exist when the distance between the chains $d = \sigma^{-1/2}$ becomes equal to R_0. For the values of P/N ($P/N > 1/\sqrt{N}$) we are mainly interested, in this work, in the frontier of the mushroom regime defined by $\sigma\sqrt{N} = 1/\sqrt{N}$.

For values of $\sigma\sqrt{N}$ higher than $1/\sqrt{N}$ we enter the wet brush regime. The interacting grafted chains

stretch away from the surface. The deformation of the brush chains has a free energy penalty associated with it since the stretched molecules have a reduced configurational entropy. In this regime, the free melt polymer chains penetrate and swell the brush, increasing in this way their entropy. The grafted chains, however, need to deform themselves to accommodate the incoming molecules and the height of the brush results from the balance between these two effects. The brush height behaves like $h = N\sigma^{1/3}P^{-1/3}$. Once again, for high enough values of P/N the repulsive interactions of the brush are screened and the brush is no longer swelled, $h = R_0 = N^{1/2}$. By equating the scaling dependencies of h on both sides, we obtain the expression $\sigma\sqrt{N} = P/N$ for the boundary line.

Finally, if we continue to increase the grafting density, we reach the dry brush regime. This regime is characterized by the progressive expulsion of the mobile chains from the grafted layer. The entropic gain associated with the penetration of the mobile P chains in the brush is not able to compensate the elastic deformation of the grafted chains. Due to the incompressibility of the melt, the height of the brush scales as $h = N\sigma$. The transition from the wet brush to the dry brush regime occurs for $\sigma\sqrt{N} = (P/N)^{-1/2}$ if $P/N < 1$ and $\sigma\sqrt{N} = 1$ if $P/N > 1$, as can be obtained from the equality of the scaling laws in the frontier region.

(i) Expulsion of the Free Chains. To give an initial picture of the behavior of the system, we show in Figure 2 the results obtained for the densities of monomers $\phi(z)$ of the grafted and mobile chains according to eqs 13, for an $N = 100$ brush. The values of σ and P are such that the system is well inside the three different regions of the diagram of states of Figure 1. For $P = 50$ and $\sigma = 0.1$ we are in the swollen wet brush regime. One can see in the full curve of Figure 2a that the grafted chains are stretched and the height of the brush is almost twice the value of the Flory radius of the coil, $R_0 = 10$. The mobile chains (dashed curve of the same figure) penetrate well inside the brush: at the wall $\phi_\alpha(z=0) = 0.03$. Figure 2b corresponds to the screened wet brush regime, $P = 150$ and $\sigma = 0.05$. The brush interactions are screened and the height of the brush is roughly equal to R_0 (full line). For this value of σ the density of monomers of the grafted chains near the wall is weak and one can find a large amount of free polymer (dashed curve) in this region, $\phi_\alpha(z=0) = 0.16$. Finally, Figure 2c shows typical density profiles of the brush (full line) and of the free chains (dashed line) in the dry brush regime, $P = 150$ and $\sigma = 0.2$. The mobile chains have been expelled from the brush $\phi_\alpha(z<11) = 0$, but the brush−melt interface has a finite thickness. The brush height is of the order of the predicted value, $h = N\sigma = 20$. In fact, despite all scaling laws for h being valid only up to a certain prefactor, it is easy to check that this factor has to be the same in all the regions of the state diagram. The numerical results show that this prefactor is roughly 1 (see for instance Figure 2b).

We have solved the SCF equations in a systematic way in order to obtain the locus of points (N, P, σ_T) that characterize the wet to dry brush transition. For a given set of values of N and P, the transition value σ_T is defined as being the value at which the free polymer density at the grafting wall $\phi_\alpha(z=0)$ becomes essentially zero. In practice we need to consider $\phi_\alpha(z=0)$ smaller than a certain ϕ_{min}. In Figure 3 we present the results

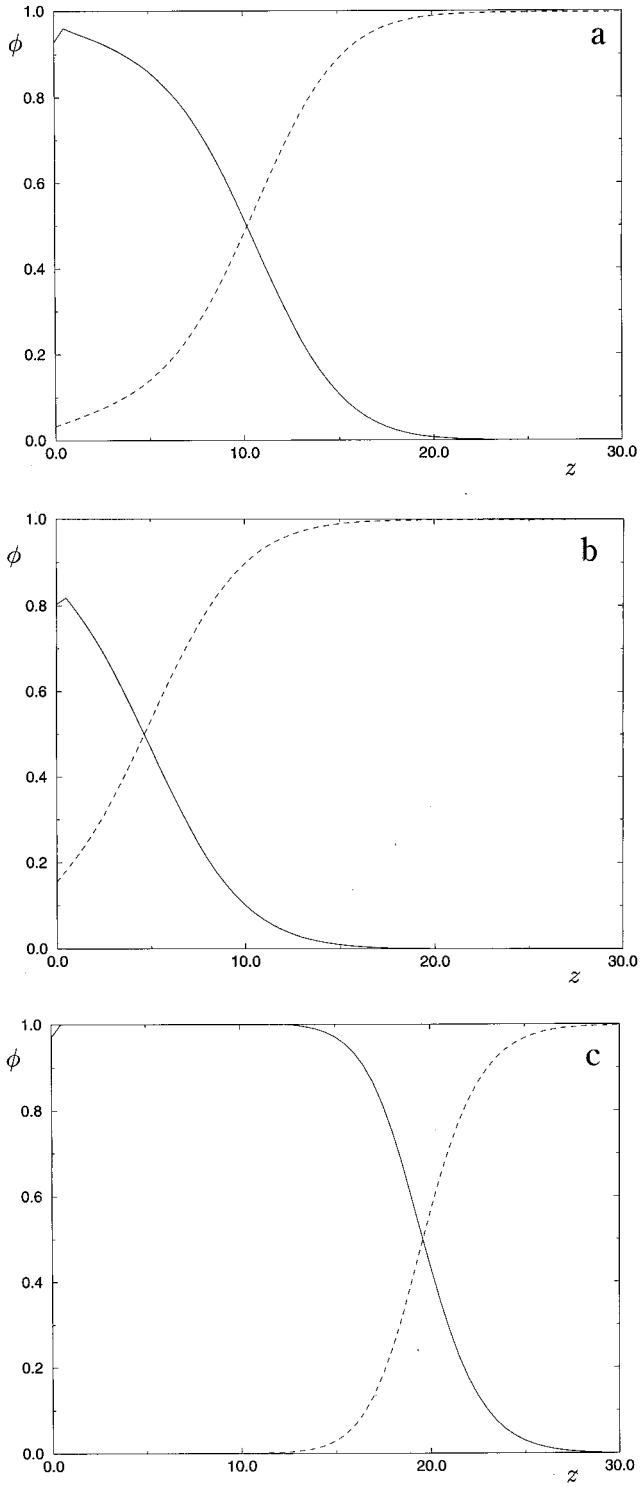

Figure 2. Grafted (full line) and mobile chains (dashed line) density profiles for an $N = 100$ brush in the three different regions of the diagram of state of Figure 1. (a)−(c) correspond respectively to $P = 50$ and $\sigma = 0.1$ in the swollen wet brush regime, $P = 150$ and $\sigma = 0.05$ in the screened wet brush region, and $P = 150$ and $\sigma = 0.2$ in the dry brush regime. See the text for discussion.

obtained for $\sigma_T\sqrt{N}$, for grafted chains with three different polymerization indices $N = 100$ (circles), $N = 200$ (squares), and $N = 400$ (triangles). For each value of N, the values of P were varied between $P = 10$ and $P = 1000$ and the SCF equations were solved at different values of σ until the transition point σ_T was found. In the same figure are also shown the scaling predictions

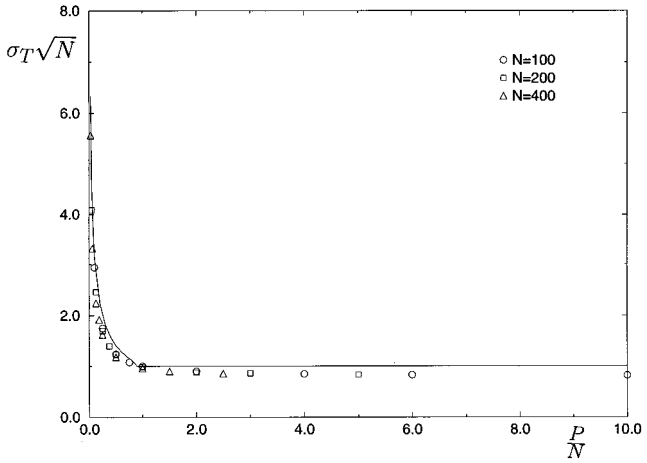

Figure 3. Locus of points (N, P, σ_T) that characterize the begining of the expulsion of the mobile chains from the grafted layer. Results are presented for $N = 100$ (circles), $N = 200$ (squares), and $N = 400$ (triangles). The solid line is the scaling prediction $\sigma_T^{scal}\sqrt{N} = (P/N)^{-1/2}$ if $P/N < 1$ and $\sigma_T^{scal}\sqrt{N} = 1$ if $P/N > 1$ of refs 12, 13, and 17.

for $\sigma_T\sqrt{N}$: $\sigma_T^{scal}\sqrt{N} = (P/N)^{-1/2}$ if $P/N < 1$ and $\sigma_T\sqrt{N} = 1$ if $P/N > 1$. The agreement between the scaling values of σ_T and the SCF numerical results is rather good. Indeed, this fact should not be surprising since it was already seen in the work of ref 13 that the SCF approximation yields values of h that are in good agreement with the scaling predictions.

(ii) Autophobicity and Attraction of Dense Brushes. The degree to which the free and the grafted chains interpenetrate is described by λ, the width of the melt−brush interface. In the wet brush regime the penetration of the mobile chains in the brush is total and λ is simply equal to the brush height, h. In the dry brush regime the free chains are expelled and the penetration is partial. If the mobile chains are short, whole molecules of the free polymer penetrate into the brush. The scaling law for λ in this region is[12,13] $\lambda = N\sigma^{-1}P^{-1}$. For large P/N only a fraction of the segments of the free chains can penetrate into the brush and the interfacial thickness behaves like[1,2,10,12,13] $\lambda = N^{1/3}\sigma^{-1/3}$. The frontier between the two regimes is $\sigma\sqrt{N} = (P/N)^{-3/2}$ (dashed line in Figure 1) that coincides with the curve predicted in refs 1 and 2 to delimit the regions of positive and negative interfacial energy between the grafted and free chains. When $\sigma\sqrt{N} > (P/N)^{-3/2}$, there exists a positive surface tension between the grafted polymer chains of the brush and the mobile chains of the bulk.[1,2] The spreading coefficient S becomes negative and a droplet of the polymer melt will dewet the brush. For σ smaller than this value, $S > 0$ and complete wetting is expected to occur.[1,2]

The criteria of the wet to dry brush transition as defined by the expulsion of the mobile chains from the grafted layer or by the crossover from a positive to a negative spreading coefficient are not equivalent. In the former case the system is wet if $\sigma\sqrt{N} < (P/N)^{-1/2}$ when $P/N < 1$ and $\sigma\sqrt{N} < 1$ when $P/N > 1$. In the latter case complete wetting is expected when $\sigma\sqrt{N} < (P/N)^{-3/2}$. We are thus lead to conclude, as in ref 12, that one part of the so-called dry brush regime of the diagram of state of Figure 1 corresponds in fact to wetting ($S > 0$) where penetration of the free chains in the grafted layer is only partial.

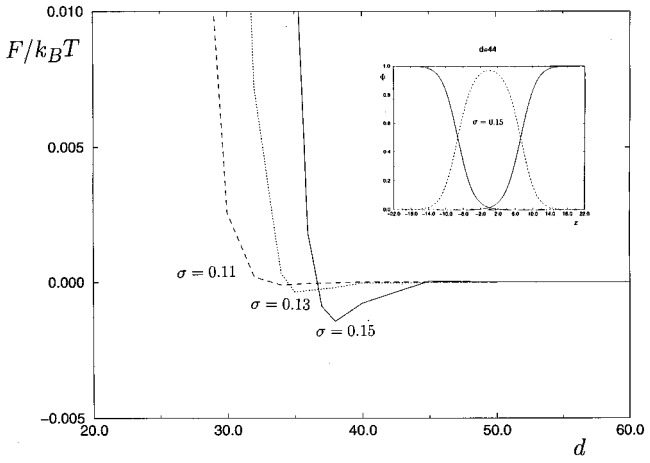

Figure 4. Free energy of interaction F/k_BT of two brushes ($N = 100$) in a melt ($P = 100$) as a function of the distance d between them at $\sigma = 0.11$ (dashed curve), $\sigma = 0.13$ (dotted curve), and $\sigma = 0.15$ (solid curve). At small separation there is a repulsive part due to the excluded volume effect between the grafted chains. The attractive part appears roughly at the contact distance of the tails of the two brushes and corresponds to the mixing of the chains with chains from the other grafted layer instead of with the free polymer chains. For $\sigma = 0.15$ and $d = 44$ (begining of the attraction) the density profiles of the brushes (solid line) and of the melt free chains (dashed line) are shown in the insert of the figure.

To confirm this idea, we need to compute the interfacial energy between the grafted and free chains and show that it changes sign according to the scaling condition of refs 1, 2, and 12. A direct computation of the interfacial energy of the system is not possible, since the numerical evaluation of the free energy of a completely dry brush raises several problems. The easiest indirect way to evaluate this energy is to compute the interaction free energy between two brushes immersed in a melt and see when this interaction becomes attractive. If we assume that it is the existence of a positive surface tension between the brush and the bulk chains that is responsible for the appearance of an effective attraction between the brushes, as described in ref 10, the two processes should be equivalent. We will see that this is indeed the case and that the effective attraction between the brushes results from the replacement of two unfavorable brush−melt interfaces by a single brush−brush interface.

In Figure 4 we present the results obtained for the free energy of interaction F/k_BT of two brushes ($N = 100$) in a melt ($P = 100$) as a function of the distance d between them, for three different values of σ. The free energy is given by[9,13,22]

$$F(d) = \sum_{i=1}^{2} \frac{\sigma \log \sigma N}{\int dz\, q_\beta(z,N)} - \int dz\, \xi(1 - \phi_\alpha(z) - \sum_{i=1}^{2} \phi_\beta(z)) \tag{15a}$$

and

$$\frac{F(d)}{k_BT} = F(d) - F(\infty) \tag{15b}$$

Equations 10 and 12−14 are solved to calculate the densities $\phi_\alpha(z)$ and $\phi_\beta(z)$ and the propagator $q_\beta(z,t)$ in the case of two brushes in contact with the melt. The only difference with respect to the problem of a single

brush in contact with a bulk melt concerns the boundary condition of the differential equation for the free chains since now at $z = z_{max}$ ($=d$) there is another brush, equivalent to the first one.

The three curves plotted in Figure 4 correspond to the three values of the grafting density $\sigma = 0.11$ (dashed curve), $\sigma = 0.13$ (dotted curve), and $\sigma = 0.15$ (solid curve). At small brush separation there is a repulsive part in the interaction free energy due to the excluded volume effect between the grafted polymers. At these small distances ($d \approx 30$ for $\sigma = 0.11$, $d \approx 32$ for $\sigma = 0.13$, and $d \approx 36$ for $\sigma = 0.15$) the two brushes compress each other and the density profiles are different from those of the very large system ($d = \infty$) for which the two brushes do not interact and $F/k_BT = 0$. In all three cases, in addition to this repulsive part there is a small attractive part, which appears roughly at the contact distance of the tails of the two brushes and corresponds to the mixing of the grafted chains with chains from the other grafted layer instead of with the free polymer chains. The density profiles of the two brushes (solid line) and of the melt free chains (dashed line) are shown for this contact distance ($d \approx 44$) when $\sigma = 0.15$ in the insert of the figure. The profiles of the two brushes are the same as those of the infinitely large system. The decrease of the distance between the brushes causes a progressive expulsion of the free chains that is observed in the density profiles and gives rise to an increasingly negative energy of interaction. The minimum of this energy is attained when the two brushes start to compress each other and a positive repulsive contribution to the energy appears. For the smallest value of the density presented, $\sigma = 0.11$, the attractive part is already so small that it can hardly be seen in the scale of the figure. For $\sigma = 0.10$ and for smaller values of σ the attractive interaction disappears.

These results for the interaction free energy are not new and were for instance observed at equivalent values of N, P, and σ in the work of ref 9. In our work we calculate in a systematic way the locus of points N, P, and σ at which the attractive interaction disappears. For fixed values of N and P, the grafting density was varied until the first value of σ, for which the free energy of interaction becomes negative, was found. The free energy was computed with accuracy to four decimal places and in some cases a few thousand iterations of the set of equations was necessary in order to attain the desired precision. The results obtained for $N = 100$ (circles), $N = 200$ (squares), and $N = 300$ (triangles) and $P/N < 1$ are shown in Figure 5. Also shown in the same figure is the solid curve corresponding to the scaling law of refs 1 and 2, $\sigma\sqrt{N} = (P/N)^{-1.5}$. The general trend of our data is well represented by the scaling prediction. However, a much better agreement can be found with the law $\sigma\sqrt{N} = (P/N)^{-2.0}$, as can be seen in the figure (dashed line).

To try to understand this slight discrepancy between the predicted values of the scaling exponents of N and P and the numerical values obtained, we investigated the region $P \gg N$ and $\sigma\sqrt{N} = 1$, for which the mean field theory of refs 1 and 2 should hold. The aproximations used in these references assume that in this region the interfacial properties of the system are already independent of P. In Figure 6 we have plotted the density profiles of two brushes with $N = 100$ and $\sigma = 0.2$, at a fixed distance $d = 48$ (that belongs to the attractive region of the interaction energy curve), for

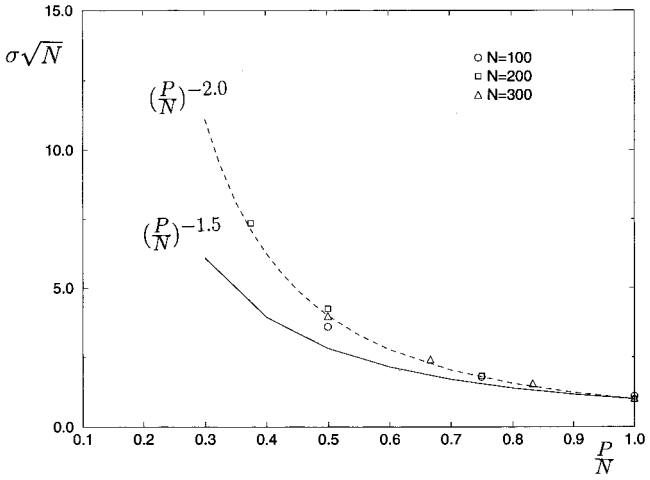

Figure 5. Locus of points (N, P, σ) at which the interfacial energy between the grafted and the free chains becomes positive. Results are presented for brushes of polymerization index $N = 100$ (circles), $N = 200$ (squares), and $N = 300$ (triangles) and for free chains with a polymerization index $P < N$. The solid line is the scaling prediction of ref 1, $\sigma\sqrt{N} = (P/N)^{-1.5}$. The dashed curve is the new scaling law $\sigma\sqrt{N} = (P/N)^{-2.0}$.

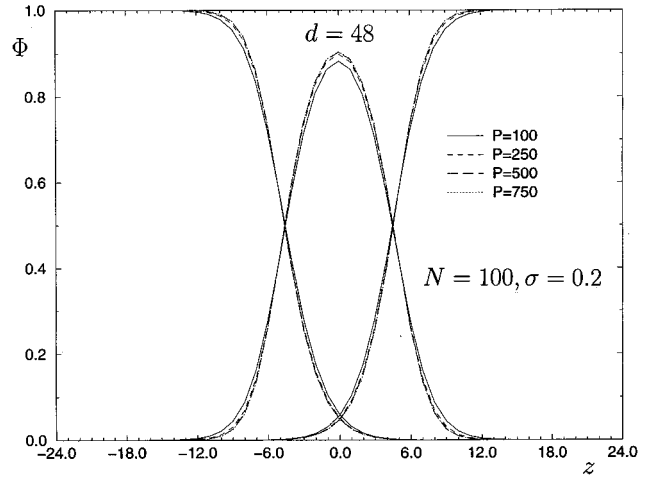

Figure 6. Density profiles of two brushes with $N = 100$ and $\sigma = 0.2$ at a fixed distance $d = 48$ (corresponding to the attractive region of the interaction free energy curve) for $P = 100$, 250, 500, and 750. The profiles start to stabilize around $P = 500$.

several values of P. For the smaller values of P presented in the figure, $P = 100$ and $P = 250$, the profiles are still changing with P and they start to stabilize arround $P = 500$. For $P = 750$ there is already no difference between the curves. This rather significant dependence of the density profiles on P is going to appear also in the calculated values of the interaction free energy, which seems to be even more sensitive to the length of the mobile chains. In Figure 7 we present the results obtained for the absolute value of the interaction free energy of two brushes with $N = 100$ and $\sigma = 0.2$, at a distance $d = 48$ for values of P that were varied between $P = 100$ and $P = 1250$. There is an asymptotic behavior of the energy in $1/P$ that cannot be described by the theory of refs 1 and 2, where terms of the order $1/P$ in the energy were neglected. This may be the origin of the differences encountered in the scaling exponents. The contributions in $1/P$ that were ignored in refs 1 and 2 are no longer negligible when the interfacial thickness is of the order of $\sqrt{P}$. For the

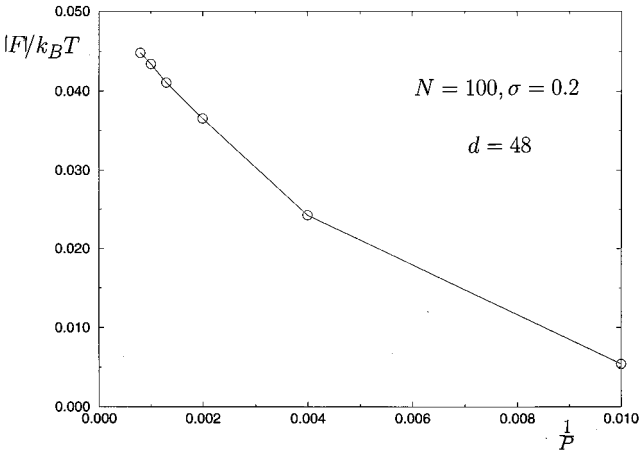

Figure 7. Absolute value of the interaction free energy of two brushes ($N = 100$, $\sigma = 0.2$) at a fixed distance ($d = 48$) as a function of $1/P$. See discussion in the text.

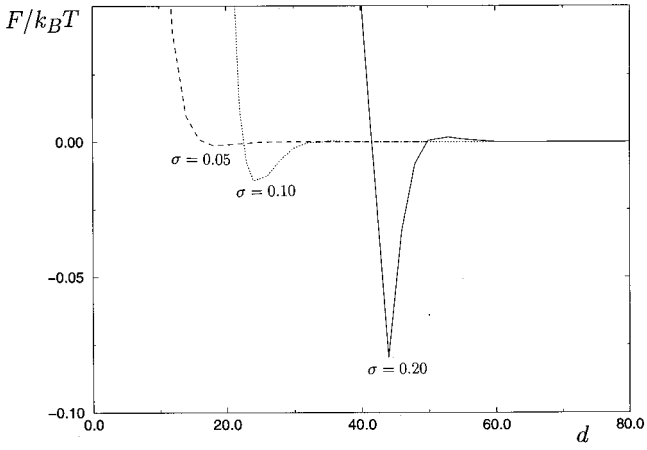

Figure 8. Free energy of interaction of two brushes with $N = 100$, immersed in a melt of $P = 200$ at three different values of σ: $\sigma = 0.05$ (dashed line), $\sigma = 0.1$ (dotted line), and $\sigma = 0.2$ (solid line).

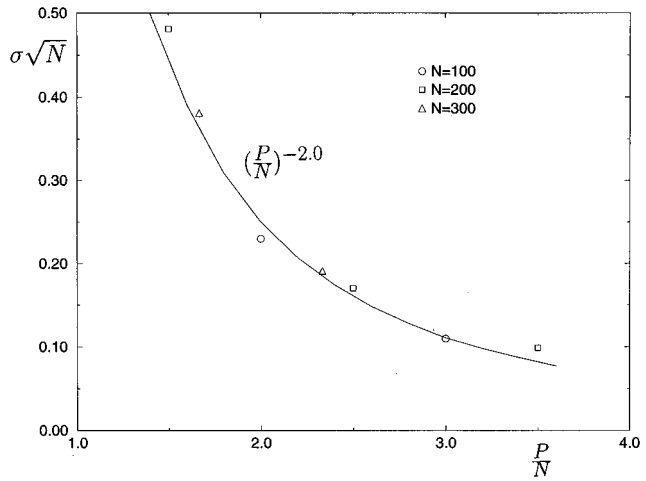

Figure 9. Crossover from a negative to a positive interfacial energy between the free and the grafted chains for $P > N$. The solid line is the new scaling law $\sigma\sqrt{N} = (P/N)^{-2.0}$. The results were obtained for brushes of polymerization index $N = 100$ (circles), $N = 200$ (squares), and $N = 300$ (triangles). The melt length P was varied betwen 200 and 700.

values of $\lambda \approx 10$ obtained with these parameters it seems reasonable that it is necessary to have a value of $P \approx 500$ in order to reach the asymptotic behavior of the density profiles in Figure 6. The same argument can be used to interpret the fact that for $P = 1000$ the asymptotic classical behavior in $\sigma^{1/3}$ expected for the mimimum of the free energy of interaction was still not attained in the work of ref 9. Indeed, not only the values of the energy are changing with P, but also the value of the distance for which this minimum is attained decreases with increasing P.

Our results clearly indicate that in the case $P/N < 1$ wetting autophobicity occurs if $\sigma\sqrt{N} > (P/N)^{-2.0}$. If $\sigma\sqrt{N}$ is smaller than this value, the spreading coefficient is positive. A droplet of the polymer melt will spread on top of the brush, partially invading the grafted layer, when $\sigma\sqrt{N} > (P/N)^{-1/2}$. When $\sigma\sqrt{N} < (P/N)^{-1/2}$, the free polymer chains penetrate completely the brush and reach the grafting wall. We can also conclude that the positive surface tension between the grafted and the free chains is indeed the mechanism responsible for the effective attraction between brushy aggregates and polymer-protected particles in a melt of long chains. An optimized dispersion (in the sense discussed in ref 9) of colloidal particles in a melt of $P/N < 1$ chains should be obtained if the grafting density is of the order of $\sigma\sqrt{N} \simeq (P/N)^{-2.0}$.

(iii) Autophobicity and Attraction of Sparse Brushes. The existence of a positive surface tension was predicted in refs 1 and 2 in the case of a melt of long chains, for a grafting density of the brush such that the system was well inside the dry brush region of Figure 1. The transition to a negative surface tension was then obtained by reducing the length P of the bulk chains by keeping the grafting density constant. Nothing is said about the related problem of going from a positive to a negative surface tension by decreasing the grafting density at a constant value of P, for $P/N > 1$. The region of screened wet brush behavior that starts at $\sigma\sqrt{N} \leq 1$ would be partialy contained inside the region $\sigma\sqrt{N} > (P/N)^{-2.0}$.

We have analyzed the behavior of the system in this new region. In Figure 8 we plot the free energy of interaction of two brushes with polymerization index $N = 100$ immersed in a melt of chains with length $P = 200$. The dashed curve corresponds to $\sigma = 0.05$, the dotted one to $\sigma = 0.1$ and the solid curve to $\sigma = 0.2$. The results are similar to those found when $P/N < 1$. Once again, there is an attractive part in the free energy of interaction at the end of the repulsive part, if σ is larger than a certain value.

Like in the case $P/N < 1$, we have calculated the set of values (N, P, σ) at which the attractive interaction disappears. The results for $N = 100$ (circles), $N = 200$ (squares), and $N = 300$ (triangles) are plotted in Figure 9 together with the corrected scaling law $\sigma\sqrt{N} = (P/N)^{-2.0}$. The melt length P was varied between 200 and 700. Our data show a very good agreement with the scaling law, indicating that also in the case $P/N > 1$ the optimum grafting density for the stabilization of colloidal particles should be described by $\sigma\sqrt{N} \simeq (P/N)^{-2.0}$. We have used the same criterion as in the case $P < N$ to define when the attractive attraction between the two brushes disappears. The behavior of the minimum of the energy in this case is, however, less well-defined than for $P < N$, in the sense that there seems to exist a residual negative part in the free energy that in practice is neglected when we truncate the values of the energies at the fourth decimal place.

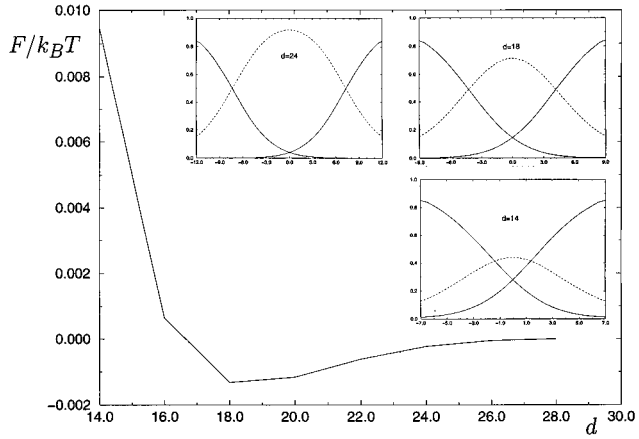

Figure 10. Interaction free energy as a function of the distance for sparsely grafted brushes ($N = 100$, $\sigma = 0.05$, $P = 200$). The density profiles of the brushes (solid line) and of the melt free chains (dashed line) are shown for the three different regions of this curve. See text for details.

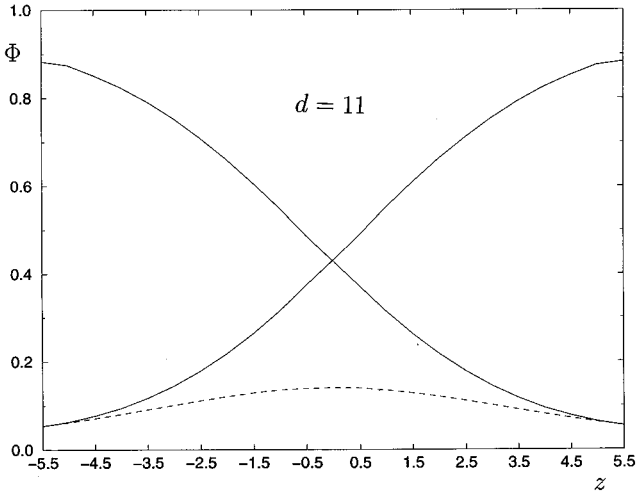

Figure 11. At small separation distances the sparsely grafted brushes interdigitate and penetrate each other and the melt free chains are expelled from the interfacial region. The density profiles of the brushes (solid line) and of the melt (dashed line) are shown for $N = 100$, $P = 200$, $\sigma = 0.05$, and $d = 11$.

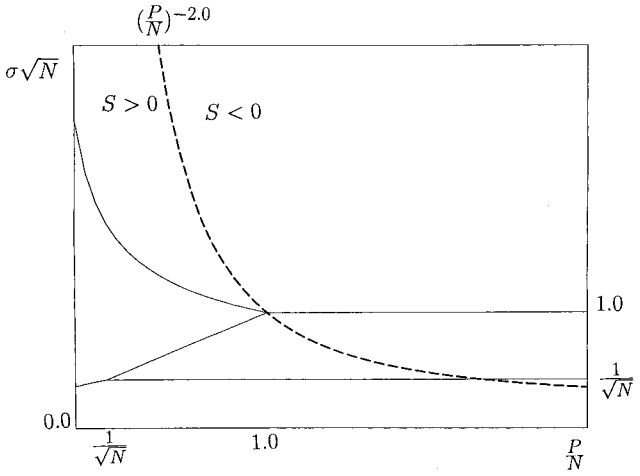

Figure 12. Diagram of state (N, P, σ) of the system. The dashed curve is the new scaling law $\sigma\sqrt{N} = (P/N)^{-2.0}$ for the crossover from a negative to a positive interfacial energy between the melt and the grafted layers.

The typical behavior of the sparsely grafted brushes in this region of the phase diagram is presented in Figure 10, for the case of two brushes with $N = 100$, $\sigma = 0.05$, and $P = 200$. These parameters correspond to a point in the screened wet brush region of the phase diagram, for which the interfacial energy betwen the grafted chains and the free chains is still positive. One can find in the figure, the density profiles of the brushes (solid line) and of the mobile chains (dashed line) at the three different zones of the curve of the interaction free energy. The distances between the brushes $d = 24$, $d = 18$, and $d = 14$ correspond respectively to the onset of attraction (and of the interdigitation of the brushes), to the minimum of the negative attraction, and to the begining of repulsion (and compression by the opposite wall). When d is decreased, free energy is gained due to the progressive expulsion of the P chains from the interfacial region, as is shown in the figure. Contrary to the dry brush regime discussed in Figure 4, brushes in this region do interdigitate and penetrate each other when this distance is reduced. This fact can already be seen in the density profiles at the distance $d = 14$ of the figure. A large part of the free P chains were already expelled from the space between the two brushes that prefer to penetrate into the opposite brush, in this way filling the space. An almost complete interpenetration of the two brushes is shown in the plot of Figure 11, for the case $N = 100$, $P = 200$, $\sigma = 0.05$, and $d = 11$. The repulsive part of the free energy of interaction in Figure 10 comes from the deformation of the brushes when they reach the opposite grafting wall. This deformation and compression of the two brushes is clearly shown by the density profiles in the case $d = 14$.

A priori there is no reason the line $\sigma\sqrt{N} = (P/N)^{-2.0}$ should stop at the frontier of the screened wet brush regime defined by $\sigma\sqrt{N} = 1/\sqrt{N}$. This is indeed the case and we have verified that in several points of the so-called mushroom regime the interfacial energy is still positive. These results are summarized in the new diagram of state of the system that is presented in Figure 12, where we plot the new frontier line between the regions of positive and negative interfacial energy.

All the possible inhomogeneities inside the planes parallel to the grafting wall, which are expected to arise in this region of very small grafting densities, where transversal density fluctuations may be very important, are completely excluded from our one-dimensional analysis of the problem. A correct treatment of this problem is beyond the scope of the present work.

IV. Conclusions

We have used the SCF approximation to carry out a systematic analysis of a polymer liquid in contact with a surface of densely grafted chains of the same polymer.

We have characterized the locus of points N, P, and σ at which the expulsion of the free polymer chains from the grafted layer begins and the interfacial energy between the grafted and the free chains becomes positive. We have shown that the two phenomena are not equivalent and occur at different regions on the diagram of state of the system. For the former phenomena (chain expulsion) the known scaling laws are shown to be quite accurate and we can say that the mobile chains start to be expelled from the brush roughly when $\sigma\sqrt{N} > (P/N)^{-1/2}$ if $P/N < 1$ and $\sigma\sqrt{N} = 1$ when $P/N > 1$. For the second phenomena (onset of autophobicity) we have

obtained the new scaling law $\sigma\sqrt{N} = (P/N)^{-2.0}$ for the crossover from a negative to a positive interfacial energy.

One of the main findings of this paper is that dewetting of the N polymer brush by the P polymer melt chains happens when $\sigma\sqrt{N}$ is larger than $(P/N)^{-2.0}$ also when P is larger than N. This implies the existence of attraction between sparsely grafted surfaces. When the surfaces are well separated, in order that each grafted layer can have an optimized height of the order of R_0, the mobile melt chains need to fill the remaining space. When the two brushes come close together, the free melt chains can be expelled and the optimized height R_0 of each of the grafted layers is obtained by interdigitation with the opposite layer.

We have shown that the positive interfacial tension between the grafted and the free polymer chains is indeed responsible for the appearance of the attractive minimum in the interaction free energy of two brushes immersed in a polymer melt. For a given set of values of N and P if $\sigma\sqrt{N}$ is larger than $(P/N)^{-2.0}$ the grafted chains do rather mix with chains from the other grafted layer than with the free polymer chains. For these values of the parameters there is an effective attraction between brushy aggregates and polymer-protected particles in a melt. Since the optimum grafting density to enhance dispersion of colloidal particles in polymer melts must be the maximum possible value of σ that yields a repulsive interaction energy between the particles, we can estimate it to be given by $\sigma\sqrt{N} \simeq (P/N)^{-2.0}$.

Acknowledgment. P.G.F. wishes to thank the support of "Programa Praxis XXI" (Portugal), through the postdoctoral fellowship BPD/4214/94.

References and Notes

(1) Leibler, L.; Ajdari, A.; Mourran, A.; Coulon, G.; Chatenay, D. In *OUMS Conference on Ordering in Macromolecular Systems, Osaka*; Springer-Verlag: Berlin, 1994.
(2) Leibler, L.; Mourran, A. *Mater. Res. Soc. Bull.* **1997**, *22*, 33.
(3) Liu, Y.; Rafailovich, M.; Sokolov, J.; Schwaerz, S.; Zhong, X.; Eisenberg, A.; Kramer, E.; Sauer, B.; Satija, S. *Phys. Rev. Lett.* **1994**, *73*, 140.
(4) Henn, G.; Bucknall, D.; Stamm, M.; Vanhoorne, P.; Jérôme, R. *Macromolecules* **1996**, *29*, 4305.
(5) Reiter, G.; Schultz, J.; Auroy, P.; Auvray, L. *Europhys. Lett.* **1996**, *33*, 29.
(6) Yerushalmi-Rozen, R.; Klein, J.; Fetters, L. *Science* **1994**, *263*, 793.
(7) Yerushalmi-Rozen, R.; Klein, J. *Langmuir* **1995**, *11*, 2806.
(8) Shull, K. *Faraday Discuss.* **1994**, *98*, 203.
(9) Hasegawa, R.; Aoki, Y.; Doi, M. *Macromolecules* **1996**, *29*, 6656.
(10) Semenov, A. *Macromolecules* **1992**, *25*, 4967.
(11) Shull, K.; Kramer, E. *Macromolecules* **1990**, *23*, 4769.
(12) Gay, G. Submitted to *Macromolecules*.
(13) Wijmans, C.; Zhulina, E.; Fleer, G. *Macromolecules* **1994**, *27*, 3238.
(14) Kerle, T.; Yerushalmi-Rozen, R.; Klein, J. *Europhys. Lett.* **1997**, *38*, 207.
(15) Binder, K.; Lai, P.; Wittmer, J. *Faraday Discuss.* **1994**, *98*, 97.
(16) Brochard-Wyart, F.; di Meglio, J.; Quéré, D.; de Gennes, P. *Langmuir* **1991**, *7*, 335.
(17) de Gennes, P. *Macromolecules* **1980**, *13*, 1069.
(18) Witten, T.; Leibler, L.; Pincus, P. *Macromolecules* **1990**, *23*, 824.
(19) Zhulina, E.; Borisov, O.; Brombacher, L. *Macromolecules* **1991**, *24*, 4679.
(20) Shull, K. *J. Chem. Phys.* **1991**, *94*, 5723.
(21) Clarke, C.; Jones, R.; Edwards, J.; Shull, K.; Penfold, J. *Macromolecules* **1995**, *28*, 2042.
(22) van Lent, B.; Israels, R.; Scheutjens, J.; Fleer, G. *J. Colloid Interface Sci.* **1989**, *137*, 380.
(23) Ferreira, P.; Leibler, L. *J. Chem. Phys.* **1996**, *105*, 9362.
(24) Hong, K.; Noolandi, J. *Macromolecules* **1981**, *14*, 727.
(25) Matsen, M.; Schick, M. *Phys, Rev. Lett.* **1994**, *72*, 2660.
(26) Doi, M.; Edwards, S. *The Theory of Polymer Dynamics*; Oxford University Press: London, 1986.
(27) Helfand, E. *J. Chem. Phys.* **1975**, *62*, 999.

MA9712460